Pergamon

Int. J. Heat Mass Transfer. Vol. 41, No. 15, pp. 2287–2295, 1998

Printed in Great Britain
0017-9310/98 $19.00+0.00

PII: S0017-9310(97)00362-1

Mass transfer properties in a grid generated turbulent flow: some experimental investigations about the concept of turbulent diffusivity

F. LEMOINE,† Y. ANTOINE, M. WOLFF and M. LEBOUCHE

LEMTA, 2, Avenue de la Forêt de Haye, BP 160, F-54504 Vandœuvre-les-Nancy Cedex, France

(*Received* 10 *June* 1997 *and in final form* 7 *November* 1997)

Abstract—This paper is devoted to the analysis of the mass transfer properties in a grid generated turbulent flow. The closure of the transport equation of the turbulent mass flux has been experimentally investigated. Two combined optical non-intrusive methods, the laser-induced fluorescence and the laser Doppler velocimetry have been used in order to measure simultaneously and instantaneously the concentration of a passive contaminant and the velocity of the flow. It has been demonstrated that the approximation production = pressure scrambling is valid over the major part of the flowfield. A model for the pressure scrambling term has been analysed in order to define a turbulent diffusivity concept. © 1998 Elsevier Science Ltd. All rights reserved.

1. INTRODUCTION

The analysis of the diffusion properties in a grid generated turbulent flow is a basic experiment which is very helpful in the understanding of the turbulent mass transfer processes. In such a flow, the turbulent field is well characterized and the hypothesis of homogeneity and quasi-isotropy can be made. The mean and fluctuating velocity and concentration field of tracers have been investigated by many authors (e.g. Nakamura *et al.* [1], Lemoine *et al.* [2], Gad-el-Hak and Morton [3], Burnage and Huilier [4], Simoens and Ayrault [5]).

The mass transport equation, under turbulent conditions, requires a closure for the concentration-velocity cross-correlation term, which is unknown. Generally, a concept of turbulent diffusivity is used [6], which is usually defined analogously to the molecular diffusion theory. In a quasi-isotropic turbulent flow, the turbulent diffusivity is defined as a proportionality constant between the mass flux transferred by turbulence and the concentration gradient. However, the literature is very poor about reliable experimental demonstrations of this concept of turbulent diffusivity. Lemoine *et al.* [2] measured the radial turbulent mass flux and demonstrated that it was proportional to the radial concentration gradient, in a grid generated turbulent flow. However, the complete understanding of the turbulent diffusivity concept requires the analysis of the transport equation of the turbulent mass flux. A quite similar work has been performed by Everitt and Robins [7], for a turbulent plane jet. These authors have analysed the concept of turbulent viscosity. All the terms of the shear stress transport equation have been investigated: the advection, production and diffusion terms are measured and the pressure-strain term is deduced through the global balance of the transport equation. The comparison between the orders of magnitude of these different terms yields a turbulent viscosity closure.

The present paper provides an experimental investigation of the advection, production and diffusion terms in the transport equation of the turbulent mass flux. The pressure scrambling term is derived from the global balance of the equation. A model is provided for the pressure scrambling term, as for the diffusion term. 2-D laser Doppler velocimetry and laser-induced fluorescence, applied to the concentration measurement [8], have been combined in order to measure simultaneously and instantaneously two velocity components and the concentration.

2. FLOWFIELD AND GENERAL CONCEPTS

The flowfield consists in a homogeneous and quasi-isotropic turbulent flow, generated by means of a grid, in a square test channel. The characteristics of the test channel and of the grid are given in ref. [2]. The passive contaminant is injected in the centre of the test channel, at 260 mm downstream of the grid, by means of a round nozzle. The injection velocity is similar to the turbulent flow velocity, in order to avoid the shear effects.

The concentration diffusion problem is axi-symmetric, and the cylindrical coordinate system (r, θ, x) can be used adequately. The velocity components are denoted U, V, W, where U, V and W are, respectively, the longitudinal, radial and orthoradial components

† Author to whom correspondence should be addressed.

NOMENCLATURE

C	molecular concentration	U	streamwise velocity component
C_c	centreline molecular concentration	V	radial velocity component.
D_t	turbulent diffusivity		
k	kinetic energy	Greek symbols	
M	grid mesh	ε	kinetic energy dissipation rate
P	pressure	ν	kinematic viscosity
(r, θ, x)	cylindrical coordinates	ρ	density
r_c	concentration profile half width radius	σ	molecular diffusivity.
$r_{\overline{vc}}$	cross-correlation profile half-width radius	Symbols	
$r_{\overline{v^2c}}$	$\overline{v^2c}$ correlation profile half-width radius	*	normalized values
U_i	velocity component in the ith direction	x	fluctuating part of X
		$\underline{X}$	instantaneous value of X
		$\overline{X}$	average value of X
		$X = \overline{X} + x$	Reynolds decomposition.

of the velocity. The Reynolds decomposition has been applied over each velocity components in order to determine the turbulent fluctuations.

The equation governing the transport of a passive scalar (molecular concentration, C) under turbulent conditions can be written with the help of the boundary layer approximation [6].

$$\overline{U}\frac{\partial \overline{C}}{\partial x} = -\frac{1}{r}\frac{\partial}{\partial r}(r\overline{vc}). \tag{1}$$

The cross-correlation between the concentration and radial velocity fluctuations $\overline{vc}$, which is the radial mass flux transferred by turbulence, is unknown: a closure appears necessary.

The transport equation of the turbulent mass flux can be written as [9]:

$$\frac{\partial \overline{u_i c}}{\partial t} + \overline{U_j}\frac{\partial \overline{u_i c}}{\partial x_j} = -\overline{u_i u_j}\frac{\partial \overline{C}}{\partial x_j} - \overline{u_j c}\frac{\partial \overline{U_i}}{\partial x_j} - \overline{\frac{c}{\rho}\frac{\partial p}{\partial x_i}} - \frac{\partial \overline{u_i u_j c}}{\partial x_j} + \sigma \overline{u_i \frac{\partial^2 c}{\partial x_j^2}} + \nu \overline{c\frac{\partial^2 u_i}{\partial x_j^2}} \tag{2}$$

where ν is the kinematic viscosity, σ the molecular diffusivity.

The flow is considered as statistically steady, and under strong turbulent conditions, the effects of the viscous dissipation and of the molecular diffusivity can be neglected. Furthermore, the turbulence is assumed to be statistically homogeneous, quasi-isotropic and the flowfield is uniform. Consequently, a few terms vanish in the transport equation:

$$\underset{(i\neq j)}{\overline{u_i u_j}} = 0; \quad \frac{\partial \overline{U_i}}{\partial x_j} = 0; \quad \underset{(i\neq j)}{\overline{u_i u_j c}} = 0.$$

Equation (2) results into two equations, respectively, along the transverse axis [equation (3)] and the longitudinal axis [equation (4)]:

$$\overline{U}\frac{\partial \overline{vc}}{\partial x} = -\overline{\frac{c}{\rho}\frac{\partial p}{\partial r}} - \overline{v^2}\frac{\partial \overline{C}}{\partial r} - \frac{\partial \overline{v^2 c}}{\partial r} \tag{3}$$

$$\overline{U}\frac{\partial \overline{uc}}{\partial x} = -\overline{\frac{c}{\rho}\frac{\partial p}{\partial x}} - \overline{u^2}\frac{\partial \overline{C}}{\partial x} - \frac{\partial \overline{u^2 c}}{\partial x}. \tag{4}$$

Generally, the closure of equation (1) consists in the definition of a turbulent diffusivity ([1, 2]):

$$\overline{vc} = -D_t\frac{\partial \overline{C}}{\partial r}. \tag{5}$$

The validation of this hypothesis can be found by analysing the orders of magnitude of the terms in equation (3).

The experimental technique, which has been fully developed in ref. [2], is able to provide the measurement of the advection term $\overline{U}(\partial \overline{vc}/\partial x)$, the production term $\overline{v^2}(\partial \overline{C}/\partial r)$ and the turbulent diffusion term $\partial \overline{v^2 c}/\partial r$. The pressure scrambling term $\overline{(c/\rho)(\partial p/\partial r)}$ will be determined by considerations of the global balance of the equation (3).

3. EXPERIMENTAL TECHNIQUE

All the important details of the experimental measurement technique are given in ref. [2]. The novelty is the possibility to obtain simultaneously the two velocity components, which requires some minor changes in the optical device.

The main component of the set-up is a 2-D laser-Doppler velocimeter (DANTEC). The passive contaminant is a fluorescent tracer, highly diluted in water. The fluorescence of the tracer, here rhodamine B, is able to be induced by the laser radiations of the velocimeter ($\lambda \approx 488$ nm and $\lambda \approx 514.5$ nm). The emitted fluorescence is proportional to the molecular tracer concentration ([8, 10]). The optical signal is collected by means of an optical device, and is sep-

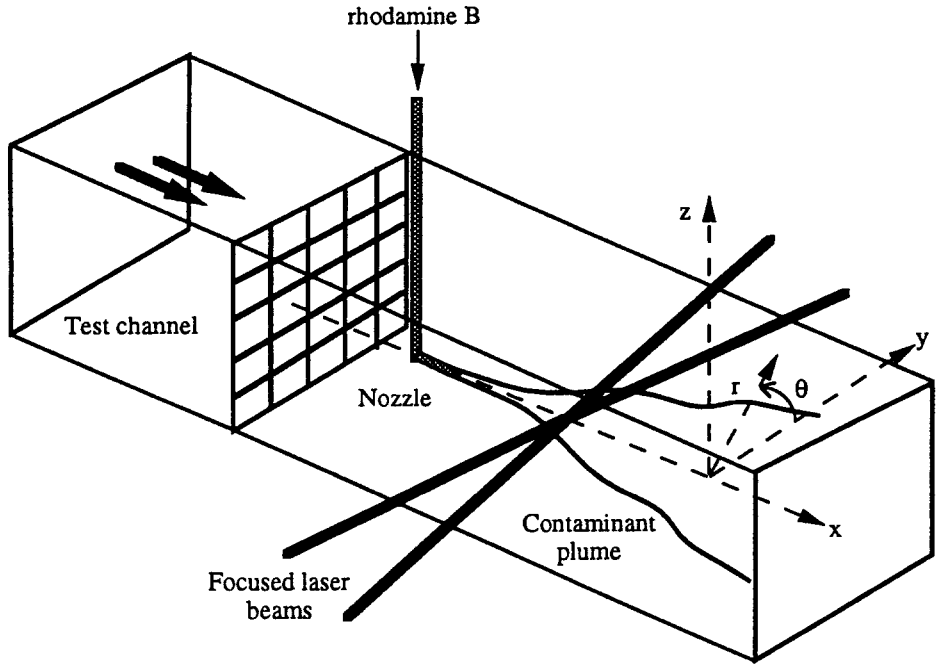

Fig. 1. Experimental arrangement.

arated and filtered subsequently. The optical signal contains:

—the scattered light at $\lambda \approx 488$ nm (filtered by a dichroic blade),
—the scattered light in $\lambda \approx 514.5$ nm (filtered by a dichroic blade),
—the larger-bandwidth fluorescence of rhodamine B (filtered by a high-pass filter, cut-off 550 nm).

The scattered light at $\lambda \approx 488$ nm and $\lambda \approx 514.5$ nm are separately processed by means of photomultiplier tubes and frequency trackers. The fluorescence intensity is measured by means of a photomultiplier tube, which provides an analogical signal, proportional to the concentration. The analogical signals, relevant to the velocity components and concentration are processed and correlated by means of an acquisition device.

4. EXPERIMENTAL CONDITIONS AND RESULTS

4.1. *Flow conditions*

The experimental flow conditions are similar to those described in ref. [2]. The only difference is that the mean flow velocity is lower (1.2 m s^{-1}). The Reynolds number, based on the mesh of the grid is $Re_M = 12\,000$. All the measurements have been performed in the range $[x/M = 35;\ x/M = 52]$, which differs also from the measurement conditions of ref. [2]. The radial measurement window is limited to 16 mm because of the size of the optical accesses (Fig. 1).

4.2. *Turbulent field*

The turbulent field is the result of the turbulent field generated by the grid and by the wake included by the injection nozzle. In the light of the measurements of the streamwise and transverse fluctuation rates, respectively, $\sqrt{\overline{u^2}}/\overline{U}$ and $\sqrt{\overline{v^2}}/\overline{U}$, reported in Fig. 2, the turbulence can be considered as quasi-isotropic and homogeneous. The turbulence level is about 3%, where the grid turbulence is correctly established, and for $x/M \geqslant 38$, the wake of the injection nozzle has vanished.

The decrease of the turbulent mean square fluctuations $\overline{u^2} \approx \overline{v^2}$ is shown in Fig. 3, in the initial area $35 \leqslant x/M \leqslant 52$. This decrease follows a power law, usually met in grid generated turbulent flows, comparable to the results available in the literature [11]:

$$\frac{\overline{U}^2}{\overline{u^2}} \approx \frac{\overline{U}^2}{\overline{v^2}} \approx 6.96\left(\frac{x}{M}\right)^{1.25}. \tag{6}$$

The kinetic energy dissipation rate ε can be estimated, since the turbulence can be considered as quasi-isotropic:

$$\varepsilon = -\frac{3}{2}\overline{U}\frac{\mathrm{d}\overline{u^2}}{\mathrm{d}x} \approx 46\left(\frac{x}{M}\right)^{-2.25}. \tag{7}$$

4.3. *Concentration field and production term*

The mean concentration field has been determined. Self-similar Gaussian profiles, comparable to those provided in ref. [2] have been found:

$$\overline{C} = C_c(x)f(\zeta) \quad \text{where } f(\zeta) = e^{-\ln 2\zeta^2} \quad (\zeta \geqslant 0) \tag{8}$$

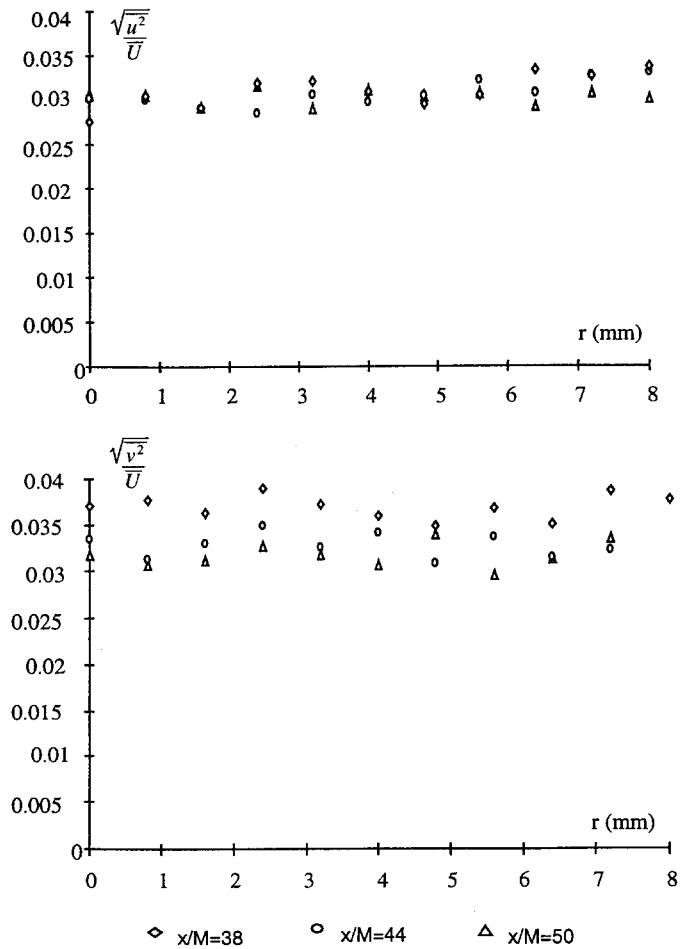

Fig. 2. Distribution of the longitudinal and radial turbulence rate over a cross-section.

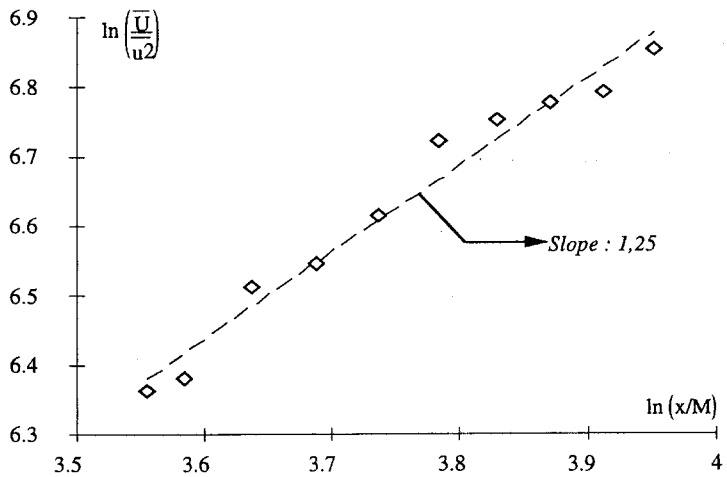

Fig. 3. Decay of the turbulent energy downstream of the grid.

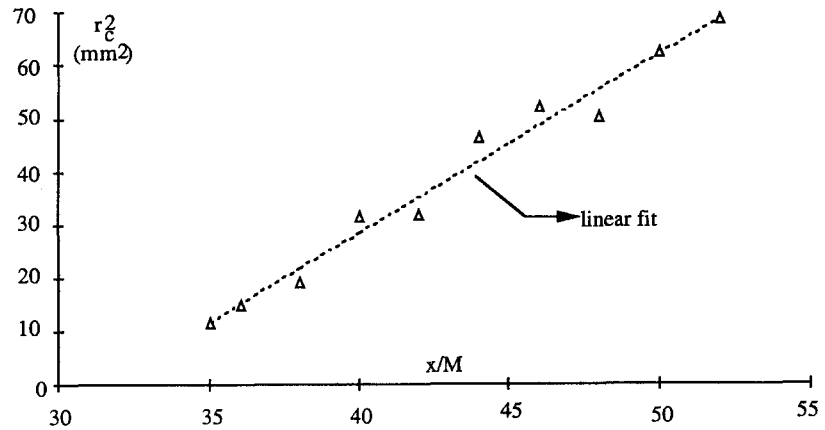

Fig. 4. Evolution of r_c^2 downstream of the grid.

where C_c is the concentration on the centreline, $\zeta = r/r_c$ and r_c is the half-width radius of the mean concentration profile.

The axial expansion of the concentration profiles downstream of the grid, reported in Fig. 4, is given by a square root law, as predicted by the theory [1]:

$$\left(\frac{r_c(x)}{M}\right)^2 = 3.35 \cdot 10^{-2} \frac{x}{M} - 0.105. \tag{9}$$

Consequently, the production team $(\overline{v^2})(\partial \overline{C}/\partial r)$ can be estimated. The radial concentration is determined by the simple derivation of equation (8):

$$\frac{\partial \overline{C}}{\partial r} = -2 \frac{C_c(x)}{r_c^2(x)} \ln 2\zeta f(\zeta). \tag{10}$$

The mean square fluctuations $\overline{v^2}$ are averaged over the cross section. Furthermore, the law of decrease of $\overline{v^2}$ downstream of the grid allows one to calculate the production term wherever in the flowfield.

4.4. *Correlation $\overline{vc}$ and advection term*

The cross correlation between the concentration and the radial velocity fluctuations have been investigated downstream of the grid. The normalized $\overline{vc}$ profiles, reported in Fig. 5, look like anti-symmetric and self similar. The radial distance is reduced by the half-width radius, denoted by $r_{\overline{vc}}$, defined in ref. [2], and the amplitude $\overline{vc}$ by the maximum value $(\overline{vc})_{max}$. In the light of these investigations, the $\overline{vc}$ profiles are given by the following self-similar law:

$$\overline{vc}^*(\zeta') = \frac{\overline{vc}(r, x)}{(\overline{vc})_{max}(x)} = g(\zeta'), \quad \text{where } \zeta' = \frac{r}{r_{\overline{vc}}}. \tag{11}$$

The distribution of $(\overline{vc})_{max}$ and $r_{\overline{vc}}$ as a function of x, downstream of the grid, are reported in Fig. 6. Numerical fits of $(\overline{vc})_{max}(x)$, $r_{\overline{vc}}(x)$ and $g(\zeta')$, have been performed in order to calculate the advection term $\overline{U}(\partial \overline{vc}/\partial x)$.

4.5. *Correlation $\overline{v^2c}$ and turbulent diffusion term*

The normalized $\overline{v^2c}$ profiles, reported in Fig. 7, exhibit a general symmetric and self-similar trend. The normalization is the following:

—the radial distance is reduced by a half-width radius, denote by $r_{\overline{v^2c}}$, defined by:

$$\frac{\overline{v^2c}(r_{\overline{v^2c}})}{\overline{v^2c}(r=0)} = \frac{1}{2} \tag{12}$$

—the amplitude is reduced by the centerline value $\overline{v^2c}$ $(r = 0)$.

Consequently, the $\overline{v^2c}$ correlation, with the help of the distribution of $\overline{v^2c}$ $(x, r = 0)$ and $r_{\overline{v^2c}}(x)$, reported in Fig. 8, can be represented wherever in the flow, by:

$$\overline{v^2c}^*(\eta) = \frac{\overline{v^2c}(r, x)}{\overline{v^2c}(r=0, x)} = h(\eta), \quad \text{where } \eta = \frac{r}{r_{\overline{v^2c}}}. \tag{13}$$

The determination of the radial gradient of the correlation $\overline{v^2c}$ yields the turbulent diffusion term $\partial \overline{v^2c}/\partial r$.

4.6. *Balance and pressure scrambling term*

Most of the terms in the turbulent flux transport equation [equation (3)] have been measured and are reported in Fig. 9 in normalized values, in the zone where the grid turbulence is well established. The pressure scrambling term $\overline{(c/\rho)(\partial p/\partial r)}$, also shown in Fig. 9, cannot be measured directly. However, it can be deduced from the global balance of equation (3). In the light of these results, one can observe that the advection and diffusion terms present the same order of magnitude, but are opposite. Consequently, the sum of the advection and diffusion terms is close to zero and vanishes from the equation (3), over the major part of the cross-section (see Fig. 9). It demonstrates that the approximation production = pressure scrambling is valid over the majority of the flow, so as to write:

$$-\overline{\frac{c}{\rho}\frac{\partial p}{\partial r}} \approx \overline{v^2}\frac{\partial \overline{C}}{\partial r}. \tag{14}$$

A model of the pressure scrambling term has been suggested by Launder [9]. Launder assumes, if the diffusion by pressure term $-\overline{(1/\rho)\partial/\partial r(pc)}$ can be ignored, that:

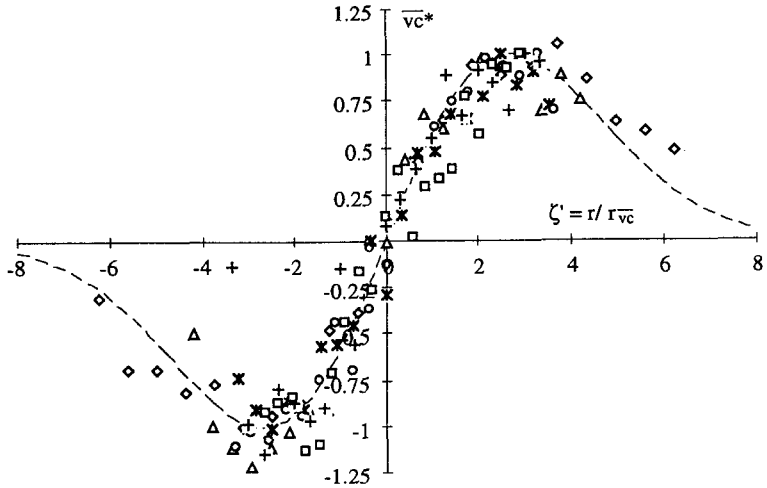

Fig. 5. Profiles of normalized radial turbulent flux over a cross-section.

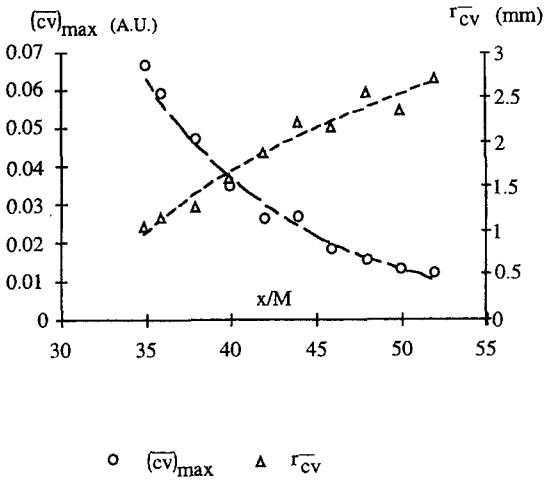

Fig. 6. Evolution of $(\overline{cv})_{max}$ and $r_{\overline{cv}}$ downstream of the grid.

$$\overline{\frac{c}{\rho}\frac{\partial p}{\partial r}} = -\overline{\frac{p}{\rho}\frac{\partial c}{\partial r}} = C_{c1}\frac{\varepsilon}{k}\overline{vc} \tag{15}$$

where C_{c1} is a constant which will be investigated.

k is the turbulent kinetic energy, which is given, for a quasi-isotropic turbulent flowfield, by:

$$k = \tfrac{3}{2}\overline{u^2} \tag{16}$$

ε, the kinetic energy dissipation rate, can be evaluated [see equation (7)]. Consequently the equations (7), (15), (16) yield the constant C_{c1}. In the light of Fig. 10, C_{c1} determined at $x/M = 52$, appears not being truly constant over the entire cross-section. As an example, a 15% variation of C_{c1} over the cross-section at $x/M = 52$ is pointed out, and this variation reaches 20% at the cross-section $x/M = 46$. This fact is probably due to the lack of accuracy in the determination of the pressure scrambling term which results from the difference of several terms. An average value of C_{c1}, between the centreline and the half-width radius r_c of the mean concentration profile has been considered. The variation of the average value of C_{c1} downstream of the grid, $C_{c1} = 4.66$ at $x/M = 46$ and $C_{c1} = 4.56$ at $x/M = 52$, is not significant.

5. CONCEPT OF TURBULENT DIFFUSIVITY

The combination of equations (14) and (15) yields the relation:

$$C_{c1}\frac{\varepsilon}{k}\overline{vc} \approx -\overline{v^2}\frac{\partial \overline{C}}{\partial r}. \tag{17}$$

The equation (17) corresponds with the usual concept of turbulent diffusivity, denoted by D_t, which is given by:

$$D_t = \frac{\overline{v^2}}{C_{c1}}\frac{k}{\varepsilon}. \tag{18}$$

Additionally, under quasi-isotropic turbulent conditions, $\overline{v^2}$, and k, and ε are constant across the transverse direction of the flowfield. The turbulent diffusivity calculated at $x/M = 52$ with the real local values of C_{c1}, reported Fig. 10 in parallel with C_{c1} is almost constant over the major part of the cross-section. However, a strong increase can be observed in the edges, probably caused by the variation of C_{c1} in this zone.

The turbulent diffusivity can be also determined directly by calculating $-\overline{cv}/(\partial\overline{C}/\partial r)$, in order to evaluate the validity of the pressure scrambling model. Another way to compare our results is to calculate the turbulent diffusivity given by Taylor's diffusion theory [6], using the concept of 'frozen turbulence'. According to this theory, the variation of the variance σ_c^2 of the mean concentration profiles is given by ([1, 4]):

$$\sigma_c^2 = \frac{2D_t}{\overline{U}}x. \tag{19}$$

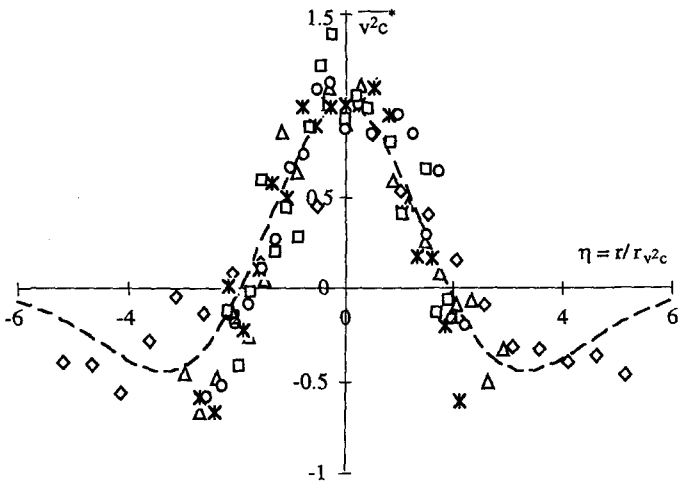

◇ x/M=38 ; △ x/M=42 ; ✱ x/M=44 ; ○ x/M=46 ; + x/M=50 ; □ x/M=50 ;

Fig. 7. Profiles of normalized triple correlation $\overline{v^2c}$ over a cross-section.

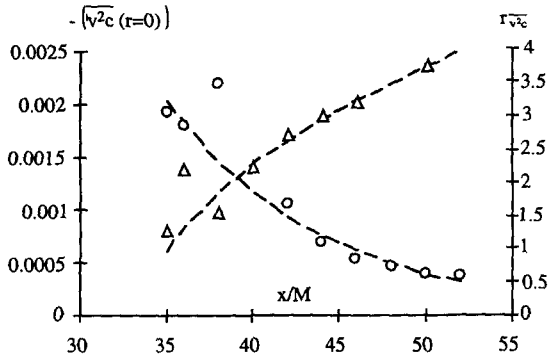

○ $-\overline{v^2c}\,(r=0)$ △ $r_{\overline{v^2c}}$

Fig. 8. Evolution of $\overline{v^2c}$ ($r = 0$) and $r_{\overline{v^2c}}$ downstream of the grid.

Assuming that the mean concentration follows a self-similar Gaussian distribution, the variance σ_c^2 can be related to the half width radius r_c by:

$$r_c^2 = \ln 2\sigma_c^2. \tag{20}$$

Consequently, Taylor's turbulent diffusivity is given by:

$$D_t = \frac{\overline{U}}{4\ln 2}\frac{dr_c^2}{dx}. \tag{21}$$

The different ways to calculate the turbulent diffusivity are reported in Fig. 11, for $x/M = 52$. The turbulent diffusivity, determined from equation (18), using the averaged C_{c1}, and by $-\overline{cv}/(\partial\overline{C}/\partial r)$ are relatively close over the entire cross-section. However, a significant difference with Taylor's turbulent diffusivity, amounting to 15%, can be observed. This difference can be probably attributed to the little anisotropy of the turbulence in such a square test channel, and to the lack of accuracy in the determination of the slope of the variation of r_c^2 as a function of x. As shown in Fig. 12, Taylor's diffusivity and the turbulent diffusivity calculated by $-\overline{cv}/(\partial\overline{C}/\partial r)$ becomes closer far downstream of the grid, where the tendency towards isotropy increases. The turbulent diffusivity calculated by equation (18) remains quasi-constant. However, the results for $x/M > 52$ must be considered with care, since they are the result of extrapolations.

6. MODEL OF THE CORRELATION $\overline{v^2c}$

A diffusion model for the triple correlation $\overline{v^2c}$ appears being reliable:

$$\overline{v^2c} = -D_{tt}\frac{\partial\overline{vc}}{\partial r}. \tag{22}$$

D_{tt} can be interpreted as a turbulent diffusivity for the turbulent flux $\overline{vc}$.

Using the turbulent diffusivity concept, the expression of the turbulent flux $\overline{vc}$ can be calculated, as shown in ref. [2]:

$$\overline{vc} = H(x)\zeta e^{-\ln 2\zeta^2} \tag{23}$$

where

$$\zeta = \frac{r}{r_c} \quad \text{and} \quad H(x) = -\frac{\overline{U}}{2}\frac{dr_c^2}{dx}\frac{C_c(x)}{r_c(x)}.$$

The $\overline{v^2c}$ expression can be derived from equations (22) and (23):

$$\overline{v^2c} = -D_{tt}\overline{U}\frac{dr_c^2}{dx}\frac{C_c(x)}{r_c^2(x)}(1-2\ln 2\zeta^2)e^{-\ln 2\zeta^2}. \tag{24}$$

In order to compare with the experimental normalized $\overline{v^2c}^*$ profiles, a similar normalization has been performed on the expression (24):

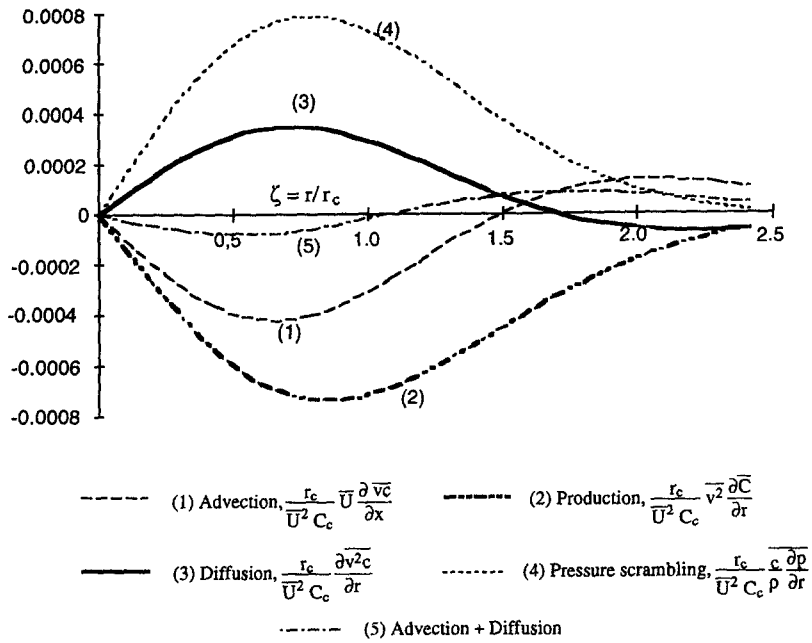

Fig. 9. Distribution of terms in turbulent mass flux transport equation over a cross-section.

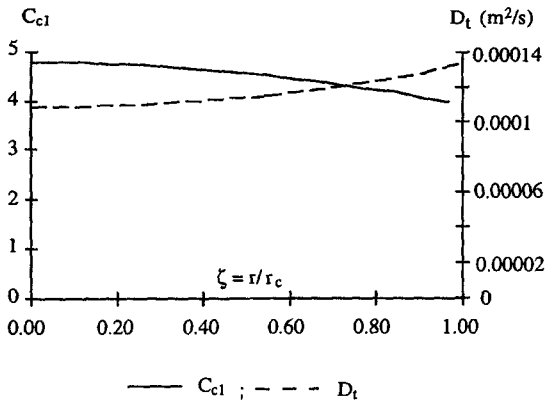

Fig. 10. Distribution of C_{c1} and D_t over a cross-section ($x/M = 52$).

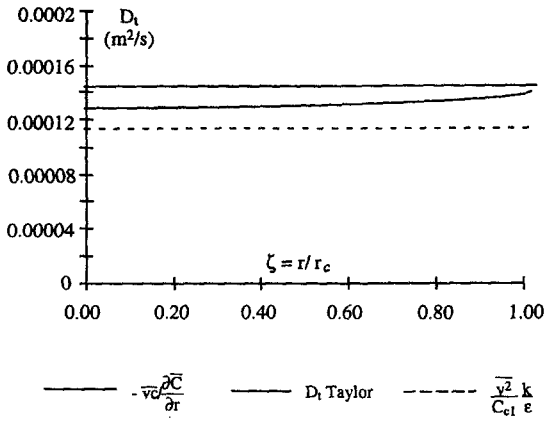

Fig. 11. Distribution of the turbulent diffusivity over a cross-section ($x/M = 52$).

$$\overline{v^2c}^* = \frac{\overline{v^2c}}{\overline{v^2c}(r=0)} = (1-2\ln 2\zeta^2)e^{-\ln\zeta^2}. \quad (25)$$

The half-width radius $r_{\overline{v^2c}}$ of the $\overline{v^2c}$ profiles, used in the definition of the reduced coordinate η, is determined by:

$$e^{-\ln 2(r_{\overline{v^2c}}/r_c)^2}\left(1-2\ln 2\frac{r_{\overline{v^2c}}}{r_c}\right)=\frac{1}{2}. \quad (26)$$

The last equation gives the only mathematically acceptable solution $r_{\overline{v^2c}} \approx 0.53r_c$, which gives $\eta = 0.53\zeta$. The experimental data show that $r_{\overline{v^2c}}$ correlates with about $0.44r_c$, but they are slightly scattered. The calculated $\overline{v^2c}^*$ profile is reported in Fig. 7 in parallel with the experimental data: a relatively good agreement between the calculated and measured $\overline{v^2c}$ profiles, over the major part of the flow is observed, which seems more than an acceptable validation of the proposed model.

7. CONCLUSION

This paper has presented the study of the diffusion mechanism in a turbulent flowfield downstream of a grid. The concept of turbulent diffusivity has been analysed.

The measurement technique based on the combined 2-D laser-Doppler velocimetry and the laser-induced fluorescence applied to the concentration measurement allowed to determine successfully the multiple correlations of the concentration and velocity fluctuations. The major part of the terms in the transport equation of the radial turbulent mass flux have been measured in order to determine their order of magnitude. The self-similarity of these terms has been

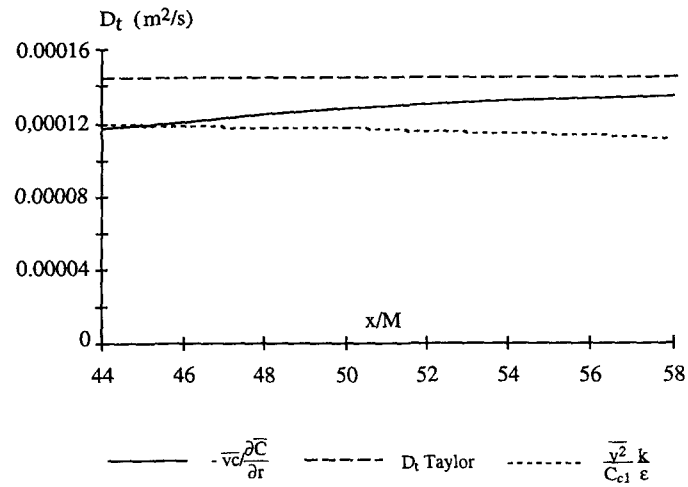

Fig. 12. Distribution of the turbulent diffusivity downstream of the grid.

pointed out. It has been shown that advection and diffusion terms have the same order of magnitude, and consequently that they counterbalance each other. One can deduce, from the transport equation of the turbulent flux, that the production and pressure scrambling terms are slightly equal. The pressure scrambling term is usually associated with a tendency towards isotropy and has been modelled as a relaxation term. As a consequence, a constant turbulent diffusivity has been defined, given by $D_t = (\overline{v^2}/C_{c1})(k/\varepsilon)$. C_{c1} is a constant which has been determined experimentally: $C_{c1} \approx 4.6$. The value of the turbulent diffusivity is about $1.4 \cdot 10^{-4}\ m^2\ s^{-1}$.

It has been also shown that the triple $\overline{v^2 c}$ can be reasonably described by a turbulent diffusion model.

Some further investigation will concern the estimation of the validity of the turbulent diffusivity concept in shear flows, such as turbulent jets for instance.

REFERENCES

1. Nakamura, I., Sakai, Y. and Miyata, M., Diffusion of matter by a non-bouyant plume in grid-generated turbulence. *Journal of Fluid Mechanics*, 1987, **178**, 379–403.
2. Lemoine, F., Wolff, M. and Lebouché, M., Experimental investigation of mass transfer in a grid generated turbulent flow using combined optical methods. *International Journal of Heat and Mass Transfer*, 1997, **40**(14), 3255–3266.
3. Gad-el-Hak, M. and Morton, J. B., Experiments on the diffusion of smoke in isotropic turbulent flow. *AIAA Journal*, 1979, **17**(6), 558–562.
4. Burnage, H. and Huilier, D., Diffusion of a submicronic spray in an homogeneous turbulent flow. *Aerosol Science and Technology*, 1990, **12**, 637–649.
5. Simoens, S. and Ayrault, M., Concentration of a scalar quantity in turbulent flows. *Experiments in Fluids*, 1994, **16**, 273–281.
6. Hinze, J. O., *Turbulence*. McGraw-Hill, 1975.
7. Everitt, K. W. and Robins, A. G., The development and structure of turbulent plane jets. *Journal of Fluid Mechanics*, 1978, **88**(3), 568–583.
8. Lemoine, F., Wolff, M. and Lebouché, M., Simultaneous concentration and velocity measurements using combined laser-induced fluorescence and laser Doppler velocimetry: application to turbulent transport. *Experiments in Fluids*, 1996, **20**, 178–188.
9. Launder, B. E., On the effect of a gravitational field on the turbulent transport of heat and momentum. *Journal of Fluid Mechanics*, 1975, **67**(3), 569–581.
10. Walker, D. A., A fluorescence technique for measurement of concentration in mixing liquids. *J. Phys. E: Sci. Instrum.* 1987, **20**, 217–224.
11. Comte-Bellot, G. and Corrsin, S., The use of a contraction to improve the isotropy of grid generated turbulence. *Journal of Fluid Mechanics*, 1966, **25**(4), 657–682.